Research Article

Check for updates

The Role of Pioglitazone Against Ehrlich Solid Carcinoma Mice Model Through Antiproliferative and Antiangiogenic Pathways

Dalia Zaafar[1*], Heba M.A Khalil[2], Soha Hassanin[3], Mohamed R. Mousa[4], Mona G. Khalil[1]

[1]Pharmacology and Toxicology Department, Faculty of Pharmacy, Modern University for Information and Technology, Cairo, Egypt; [2]Veterinary Hygiene and Management Department, Faculty of Veterinary Medicine, Cairo University, Giza, 12211, Egypt; [3]Biochemistry Department, Faculty of Pharmacy, Modern University for Information and Technology; [4]Pathology Department, Faculty of Veterinary Medicine, Cairo University, Giza, 12211, Egypt.

Abstract | **Background:** Cancer is one of the leading causes of death and morbidity worldwide, and it is linked to a variety of genetic and hormonal factors. Patients frequently experience cancer metastasis, relapse, and therapeutic failure despite the use of advanced therapeutic strategies for cancer treatment. As a result, many scientists are currently looking for newly repositioned drugs that can either inhibit cancer proliferation or promote cancer cell apoptosis. **Methods:** This study examined the effectiveness of pioglitazone (Pio) against mice bearing Ehrlich solid carcinoma in terms of its ability to inhibit cell proliferation and angiogenesis. Six groups were created using sixty male mice after the Ehrlich inoculation tumor growth was confirmed: control, Cis (5 ml/kg), Pio low dose (LD) (17.5 mg/kg), Pio high dose (HD) (30 mg/kg), Cis+Pio LD, and Cis+Pio HD. Different parameters, including behavioral, biochemical such as malondialdehyde (MDA), reduced glutathione, superoxide dismutase (SOD), tumor growth factors, and apoptotic TUNEL assay, were evaluated after three weeks in addition to Immunohistochemical analysis was done on the proliferating cell nuclear antigen (PCNA), hypoxia-inducible factor 1-alpha (HIF-1), PPAR, and cyclin D1. **Results:** Mice treated with Cis+Pio HD showed higher levels of SOD, GSH, p-ERK1/2 and p38-MAPK, as well as lower levels of MDA and tumor growth factor beside the higher apoptotic activity. Furthermore, Cis+Pio HD reduced the expression of PCNA and HIF-1 and increased the expression of PPARγ, which improved the histopathological changes. **Conclusion:** Pio possesses ESC-specific anticancer abilities. However, more research is needed before it can be used as an adjuvant agent to boost the therapeutic efficacy of chemotherapy in the treatment of many types of cancer.

Keywords | Pioglitazone; Cisplatin; Ehrlich solid carcinoma; Oxidative stress; VEGF; PPARγ; anticancer agents; tumorigenesis; biochemical indices

INTRODUCTION

Cancer is the second prominent cause of death globally, also prevalence is expected to increase by 2040 due to the increase in the new cases of malignancy annually (Bray et al., 2018). Chemotherapeutic medications are extensively used in cancer treatment either alone or with radiotherapy and surgical interventions. Cisplatin, one of the antineoplastic alkylating agents, has a significant proven efficacy against many types of malignancies, such as the neck, ovaries, testes, and lung cancers (Al-Eitan et al., 2020). However, despite its substantial antineoplastic

effectiveness, cisplatin often causes toxicity to several body organs, such as the kidney, liver, stomach, bone marrow, and hair (Ekinci et al., 2017). Moreover, cancer drug resistance is observed in many patients treated with cisplatin and then relapsed after the treatment regime.

Furthermore, some pharmaceutical agents' antineoplastic activity, primarily prescribed for other treatment purposes, are currently been researched. (Pantziarka et al., 2018). The main advantages of these agents are that: first of all, they have well-known pharmacokinetic properties. Secondly, they have a known toxicological profile and are available in the market (approved by the FDA) (Elkhawaga et al., 2019).

Recent evidence suggests that anti-diabetic drugs, such as metformin and thiazolidinediones (TZDs) compounds have a proven efficacy in combating carcinogenesis (Choi and Roberts, 2016). One of the TZDs, pioglitazone is an oral insulin-sensitizing agent prescribed primarily to treat diabetes mellitus type 2. It acts as an agonist of the peroxisome proliferator-activated receptor (PPARγ), which is highly expressed in human adipose tissue. In addition, PPAR-γ has a crucial role in cellular proliferation, apoptosis, and tumorigenesis (Higuchi et al., 2019). Extensive research has shown that pioglitazone, a PPARγ agonist, possesses anti-cancer activity against many cancer models (Ciaramella et al., 2019, Dana et al., 2019). Also, it reduces drug resistance when combined with chemotherapeutic drugs like doxorubicin and cisplatin (Higuchi et al., 2019, Higuchi et al., 2020). However, many studies argued that pioglitazone might increase cancer incidence in human body organs, such as the urinary bladder, pancreas, and prostate (Tang et al., 2018, Wen et al., 2018).

These studies' results are somewhat controversial, and there is no general agreement about pioglitazone's safety as a chemo-adjuvant agent. Besides, the debatable results regarding pioglitazone, and their impacts on the sickness behavior usually associated with chemotherapy- and radiotherapy-treated patients have not been elucidated. Sickness behavior includes various symptoms ranging from anorexia, lethargy, and locomotion disturbance to depression and cognitive impairment. It was confirmed in many rodent cancer models like mammary tumors and oral cancer (Bever et al., 2017).

PRIMARY ENDPOINT
This research was performed to investigate the actual effect of pioglitazone on tumor angiogenesis and proliferation associated with the possible molecular pathways and histopathological changes during pioglitazone treatment alone or combined with cisplatin in ESC-bearing mice.

MATERIALS AND METHODS

The impact of pioglitazone on sickness behavior of ESC-bearing mice was assessed, including feed intake, body weight, tumor volume, locomotion, and anxiety-like behavior. In our study, we used the ESC model, a form of spontaneous murine adenocarcinoma in all mice strains. This model is characterized by rapid proliferation in any mouse and is easily available, making it useful in chemotherapy research.

ANIMAL HOUSING AND ETHICAL STATEMENT
Sixty male *Swiss* mice (25–30 g) were selected as the animal model to induce solid Ehrlich tumors. Mice were purchased from the National Cancer Institute (Cairo, Egypt) and acclimatized for one week before starting the study. They were kept in a standard laboratory setting (25°C; 50% humidity; light/dark; 12/12 h cycle), Mice were administrated a calculated amount of balanced commercial diet (50 g) and water was readily available. All experimental procedures were following NIH Guidelines for the Care and Use of Laboratory Animals and approved by the Institutional Animal Care and Use Committee (Vet-IACUC, Approval No: CUIIF1021) of Cairo University, date of approval April, 2021.

EHRLICH SOLID CARCINOMA MODEL
The Ehrlich ascites carcinoma (EAC) cell line was obtained from a stock female mouse bearing ascitic fluid and then diluted with normal saline (1:10). ESC was induced by intramuscular injection of 0.2-ml ascitic fluid in the right thigh of each mouse's hind limb. The number of cells was 2.5×10^6 EAC cells per 0.2-ml ascitic fluid (Noaman et al., 2008).

EXPERIMENTAL STUDY
On day eight post-inoculation of ESC, tumor growth was confirmed by visualizing a solid mass growth in each mouse's right thigh. Then six groups of ten mice were randomly selected as follows: Group (1) (untreated control): mice were gavaged water (5 ml/kg), group (2) (Cis group): mice were injected i.p with cisplatin (5 mg/kg every six days), (Zhao et al., 2015), group (3) (Pio LD): mice were gavaged with a low dose of pioglitazone (17.5 mg/kg/day), group (4) (Pio HD): mice were gavaged with a high dose of pioglitazone (30 mg/kg/day), group (5) (Cis+Pio LD): mice treated with a combination of cisplatin (5 mg/kg every six days, I.p), and pioglitazone (17.5 mg/kg/day, p.o.), (Al-Muzafar and Amin, 2018), group (6) (Cis+Pio HD): mice treated with a combination of cisplatin (5 mg/kg every six days, I.p) and pioglitazone (30 mg/kg/day, p.o.) (Kubota et al., 2006). All treatments were launched on day eight and continued for 21 days (a three-week therapeutic period).

Justification of pioglitazone doses

The low and high doses of pioglitazone were previously used in studies. (Kubota et al., 2006; Lamontagne et al., 2013; Al-Muzafar and Amin, 2018). Two different doses were used to clarify whether the expected antiangiogenic and antiproliferative effects of pioglitazone are dose-dependent or not.

The maximal human treatment dose of pioglitazone for the treatment of hyperglycemia is 45 mg, usually given once daily. In this study, two different doses of pioglitazone (17.5 and 30 mg/kg) was used, and the Reagan–Shaw method can be used to calculate the human equivalent dose (Reagan-Shaw et al., 2008). Human equivalent dose (mg/kg) = animal dose (mg/kg) x animal (km)/human (km). Km is equal to 37 for a 60 kg adult human and 3 for a 20 g mouse. As a result, for a 60-kg adult, the human dose equivalents of 17.5 mg/kg and 30 mg/kg are 84 mg and 144 mg, respectively. This study's doses are therefore higher than the highest antihyperglycemic dose already recorded for humans.

Feed intake, body weight, tumor volume, and mortality rate

Feed intake of ESC-bearing mice was calculated daily by administering a weighted food in the feed hopper and then measuring the leftover on the next day. Body weights were also measured weekly. The tumor volume was taken every eight days using a digital caliper and calculated from the following equation tumor volume $(mm^3) = 0.52\ AB^2$, A and B are the minor and major axis, as reported previously (Ali et al., 2022). Also, the mortality rate was recorded throughout the experimental period.

Behavioral testing

After the last dose of drugs, mice were submitted for behavioral assessment as follows:

Open field test: The open field test was used to investigate the locomotor activity of mice as described by Khalil and colleagues (Khalil et al., 2021). Briefly, the mouse was positioned in the corner of a wooden box (70 × 70 ×35 cm) with the floor divided into 16 equal squares. The mouse was allowed to explore for 3 min, and the number of squares crossed by all mouse paws as well as the rearing frequency were recorded.

Elevated plus-maze: After the open field test, mice were subjected to the elevated plus-maze test to measure the anxiety-like behavior as illustrated by Hamdan and colleagues (Hamdan et al., 2020). Briefly, the mouse was positioned in the center of the elevated plus-maze facing the open arm. The maze was wooden and composed of two open and two closed arms (50 × 10 × 30 cm) and was elevated 60 cm above the floor. The mouse was allowed to explore the maze for 5 min, and the numbers of open and closed arm entries were counted. Also, the time spent by the mouse in the open and closed arms was recorded. Finally, the devices were cleaned with diluted alcohol between each session to remove any olfactory cues.

Euthanasia and tissue sampling: Twenty-four h after the last behavioral test, blood was collected from the mice's orbital canthus of the eye, and serum was separated. Then mice were euthanized by anesthesia with a mixture of ketamine (Dopalen 300 mg/kg, i.p.) and xylazine (Anasedan 30mg/kg, i.p.) followed by cervical dislocation. The right thigh was excised and divided into two halves. Half was preserved in neutral buffer formalin, and the second half was stored in −80°C for further biochemical analyses.

Biochemical analysis

Redox status assay

Estimation of Glutathione levels: Determination of GSH levels was done according to the method described by Hissin and colleges. (Hissin and Hilf, 1976). Because o-phthalaldehyde reacts with GSH in the assay to produce fluorescence, it's able to quantify GSH accurately. The test was done using Glutathione Fluorometric Assay Kit (Catalog #K264-100, BioVision, USA). The procedure was done according to the instruction of the manufacturer using a fluorescence plate reader equipped with Ex/Em = 340/420 nm.

Estimation of Lipid peroxidation (MDA): the amount of malondialdehyde (MDA) formed during the thiobarbituric acid reaction method was used to determine lipid peroxidation (LPO) levels in the samples according to Ohkawa and colleagues (Ohkawa et al., 1979). The assay was done using lipid peroxidation colorimetric assay kit (Catalog #K739-100, Biovision, USA) according to the manufacturer instructions. Thiobarbituric Acid reacts with MDA in the sample to form the MDA-TBA adduct, which can be measured colorimetrically. Absorbance was read at wave length 532 nm.

Estimation of Superoxide Dismutase (SOD) activity: Method used for measuring SOD activity according to Nishikimi and colleagues (Nishikimi et al., 1972). The sensitive SOD assay kit utilizes WST-1 that produces a water-soluble formazan dye upon reduction with superoxide anion. The rate at which a superoxide anion reduces xanthine oxidase is linearly related to that enzyme's activity, and SOD inhibits it. SOD's antioxidative activity can be measured. colorimetrically. Using a microplate reader, the absorbance was read at 450 nm. The assay was done using superoxide dismutase activity assay kit (Catalog #K335-

100, BioVision, USA). The procedure was done according to the manufacturer instructions.

Tumor growth factors and proliferation assay

As markers for angiogenesis, vascular endothelial growth factor (VEGF) and epidermal growth factor (EGF) were estimated in serum samples using chemiluminescent immunoassays, which were performed according to the instructions of Cloud-Clone Corp, USA, with catalog numbers (#SEA143Mu) and (SCA560Mu), respectively. Reactions were assessed by measuring the optical density using an automated ELISA reader (SpectraMax ® M5, Molecular Devices, United States) at 450 nm.

TUNEL assay

The tumor cells were divided into 5 × 5 mm sections and fixed by immersion in PBS containing 4% paraformaldehyde for 24 h at 4°C. Tissue Path was used to embed the fixed tissue (Curtin Matheson Scientific Inc.). The TUNEL assay was carried out according to the manufacturer's instructions provided by Vanzyme (A111, Nanjing, China) on 4 m tissue sections prepared with a microtome. Apoptosis in tumor sections was quantitated by counting the number of TUNEL-positive cells in 30 random microscopic fields. Images were acquired by fluorescence microscopy (IX61, Olympus, Japan). Cells were considered positive if they were stained bright-green.

Western blotting

Tumor tissue lysate was prepared for Western blotting with lysis buffer containing 50-mM Tris-HCl, 150-mM NaCl, 1-mM EDTA, 1-mM EGTA, pH 7.8, and 1% Triton X100 supplemented with sodium orthovanadate, sodium pyrophosphate, protease inhibitor cocktail, and PMSF. The antibodies used are as follows: IGF-1 (Novus biologicals, Canada), p38 MAPK (Health signaling technology, USA), PPARγ (Santa Cruz, USA), p-ERK ½ (Mybiosource, USA). Protein bands intensity was normalized to beta-actin, measured using Image J software (ImageJ 1.45s, NIH, USA), and the data were expressed in terms of percent relative to controls.

Histopathological examination

For the preparation of stainable tissue sections, the formalin fixed samples were passed in different grades of alcohols for dehydration followed by clearing in three changes of xylenes and finally passed in three changes of melted paraffin wax. After embedding and molding 5 μm sections were cut and stained with hematoxylin and eosin (H&E) (Bancroft and Gamble, 2013). The extension of the necrotic area was measured and mitotic figures were counted in 10 high- power fields and mean was calculated for each sample (Gardouh et al., 2018). All histologically stained sections were photographed using a digital camera (Leica

DMC 4500, Germany) coupled to a digital light microscope (Leica DM4 B, Germany).

Immunohistochemical examination

Paraffin tissue sections of the resected tumor were cut to a 5-μm thickness then mounted on poly-l-lysine coated slides. After deparaffinization and rehydration steps, slides were exposed to an antigen retrieval step that was conducted in sodium citrate buffer (10mM Sodium Citrate, 0.05% Tween 20, pH 6.0) at the microwave for 15–20 min. Non-specific staining was reduced via treatment with 1% bovine serum albumin in PBS for one h. After washing, slides were incubated with anti-PCNA (1:200, SC-56, Santa Cruz Biotechnology, Inc), anti- HIF-1α (1:200, sc-13515, Santa Cruz Biotechnology, Inc), anti-PPARγ (1: 200, sc-7273, Santa Cruz Biotechnology, Inc), and anti-Cyclin D1 (1: 200, sc-8396, Santa Cruz Biotechnology, Inc) overnight at 4°C. Slides were washed and incubated with HRP-labeled goat anti-mouse secondary antibody (1:500, ab97023, Abcam Inc.) for 1 h at room temperature. Then the sections were rinsed with PBS and incubated with diaminobenzidine (DAB) for 5 min. Hematoxylin was used as counterstain. The negative control step was applied via deletion of primary antibody incubation. Positive immune staining was assessed as the area percentage of expression in 10 microscopic fields in each section using Cellsens dimination software (Olympus, Tokyo, Japan), and the mean was calculated for each group (Ezzat et. al., 2022).

Statistical analyses

First, Shapiro–Wilk normality test was conducted to check if the data met the requirements of satisfying normality and homogeneity of variance then One-way analysis variance (ANOVA) followed by Bonferroni post hoc test was applied to compare the different groups. For the western blotting results that failed the normality test, non-parametric Kruskal–wallis test followed by Dunn's methods was performed. The data are presented as means ± standard deviation (SD). Statistical analysis was performed using the statistical package SPSS v.24 (software; SPSS Inc., Armonk, NY, USA) (Stehlik-Barry and Babinec, 2017). The significance level for all tests was set at $P \leq 0.05$.

RESULTS

Effect on feed intake, body weight, tumor volume, and mortality rate of ESC mice

There was an increase in the feed intake in the Pio (LD) and Pio (HD) treated mice compared to other experimental groups; however, nonsignificant. There was no significant difference in the initial body weight of all ESC-bearing mice. While there was a considerable increase in the body weights of Pio (LD), Pio (HD), and Cis+Pio (HD) treated mice compared to cisplatin-treated mice. Regarding

Table 1: Effect of cisplatin and pioglitazone combination on feed intake, body weight, tumor volume, and mortality rate of ESC mice

Group	Untreated control	Cis	Pio (LD)	Pio (HD)	Cis+Pio (LD)	Cis+Pio (HD)
Feed intake (g)	3.41±063	5.0±2.23	7.7±1.43	6.04±0.51	4.93±1.08	4.16±0.77
Initial body Wt. (g)	36.67±1.66	33.33±1.05	36.67±1.05	36.67±2.10	31.67±1.05	34.29±2.29
Final body Wt. (g)	29.00±1.87	22.50±1.44	35±00@	36 ±2.9@	27.50 ±1.44	31.67±2.10@
Tumor volume at 8th day (mm³)	454.82±117.2	156.17±18.6*	248.9±32.49	347.3±51.10	228.7±33.69	249.6±17.96
Tumor volume at 16th day (mm³)	1027.6±314.4	349.78±73.4*	576.5±74.36	341.43±96.8	286.08±12.7*	661.4±127.36
Tumor volume at 21th day (mm³)	1015.2±189.26	299.6±125.1*	549.98±98.16	725.08±76.82	310.65±54.9*	572.65±98.16
Mortality %	0	40%	0	0	30%	10%

Data are expressed as mean ± SD, one-way ANOVA followed by post hoc test Bonferroni test for ten mice in each group. * Significant from the untreated control group, and @ Significant from the cisplatin group, $p<0.05$. For mortality rate, data are expressed as a percentage

tumor volume, it tends to decrease significantly in the Cisplatin and Cis+Pio (LD) treated mice compared to control mice over the experimental period. Concerning the mortality rate, there was no difference in the mortality rate between Untreated control, Pio (LD) and Pio (HD) treated mice compared to other experimental groups, no mortalities detected in these groups. On the other hand, the mortality rate reached 40 % in Cisplatin, 30 % in Cis+-Pio (LD) treated mice, and 20% in Cis+Pio (HD) treated mice (Table 1).

EFFECT ON LOCOMOTOR ACTIVITY AND ANXIETY-LIKE BEHAVIOR OF ESC MICE

No significant difference in the locomotor activity visualized by the number of crossing squares and the frequency of rearing activity between different groups. However, there is a tendency to increase in the rearing activity of Cis+Pio (LD), and Cis+Pio (HD) treated mice as compared to cisplatin-treated mice and untreated controls (Fig. (1) a,b). Concerning anxiety-like behavior in the elevated plus-maze, there was no significant difference in the open arm duration, open arm entry frequency, close arm duration, close arm entry frequency. However, there was a decrease in the open arm duration and entries in the cisplatin-treated mice compared to other groups. Also, the Pio (LD), Pio (HD), Cis+Pio (LD), and Cis+Pio (HD) treated mice spent more time with more frequency in the open arms as compared to cisplatin-treated groups (Fig (2) a, b). On the other hand, cisplatin-treated mice spent more time in closed arms than different experimental groups (Fig (2) c, d).

EFFECT ON ANTIOXIDANT ACTIVITY

This study revealed that, the Pio (30 mg/kg) group had the highest levels of SOD compared to other groups, then fol-

lowed by the Cis+Pio (HD) group. In the case of GSH, the Pio (LD), Pio (HD), Cis+Pio (LD), and Cis+Pio (HD) groups had significantly higher levels compared to both untreated controls and cisplatin group.
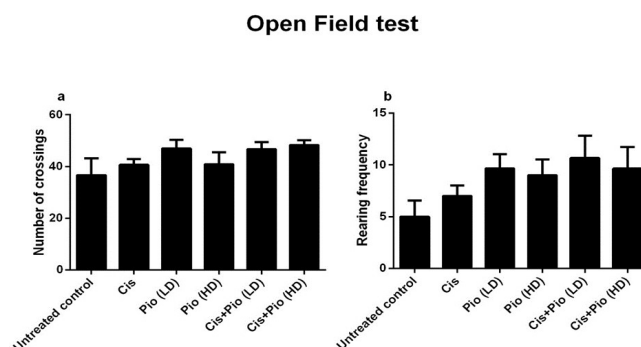

Figure 1: Effect of pioglitazone on the locomotor activity of ESC-bearing mice in the open field test. a. Number of crossings, and b. Rearing frequency. Data are expressed as mean ± standard deviation (SD), (one-way analysis of variance (one-way ANOVA).

Pioglitazone in both doses had a significant lower MDA levels compared to cisplatin. In contrast, the Cis+Pio (LD) group did not differ from the cisplatin group. However, the Cis+Pio (HD) group showed the lowest levels of MDA significantly (Fig (3)).

EFFECT ON GROWTH FACTORS AND PROLIFERATION

Concerning VEGF, both Cis and Cis+Pio (LD) groups had similar VEGF levels. The group Pio (LD), Pio (HD), Cis+Pio (HD) had lower VEGF levels when compared to the Cis group.

These results revealed that the groups Pio (LD), Pio (HD), Cis+Pio (LD), and Cis+Pio (HD) had significant lower

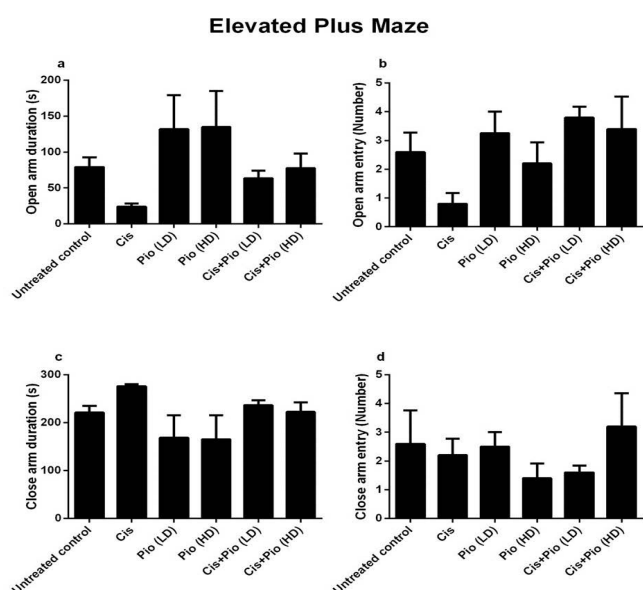levels of IGF-1 when compared to both untreated controls and Cis group.

Elevated Plus Maze

Figure 2: Effect of pioglitazone on the anxiety-like behavior of ESC-bearing mice in the elevated plus maze. a. Open arm duration, b. Open arm entry, c. Close arm duration, and d. Close arm entry. Data are expressed as mean ± standard deviation (SD), (one-way ANOVA), p<0.05
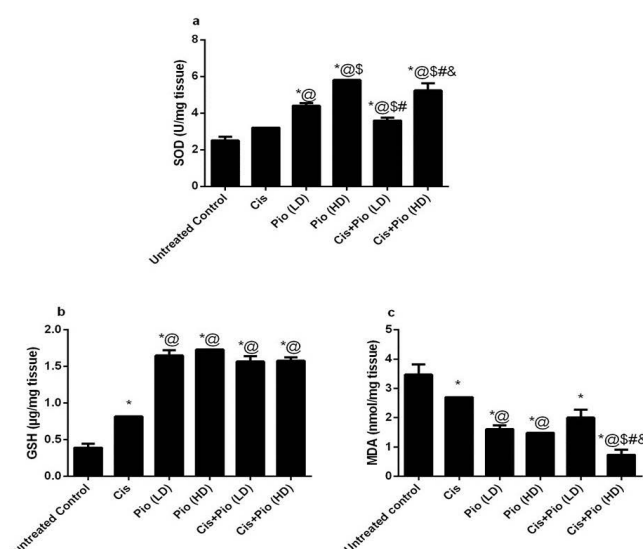

Figure 3: Effect of pioglitazone on the redox status of ESC-bearing mice. a. Superoxide dismutase (SOD), and b. Reduced glutathione (GSH), and c. Malondialdehyde (MDA). Data are expressed as mean ± SD, one-way ANOVA followed by post hoc test Bonferroni test for ten mice in each group. * Significant from the untreated control group, @ Significant from the cisplatin group, $ Significant from the Pio (LD) group, # Significant from the Pio (HD) group, & Significant from the Cis+ Pio (LD) group, p<0.05.

The EGF results highlighted that pioglitazone in both doses in addition to Cis+Pio (HD) lowered EGF levels significantly than that of untreated control and Cis group. The Cis+Pio (LD) group was lower in IGF-1 levels than the Cis group; however, it had higher IGF-1 levels than pioglitazone only (Fig (4) a–c).
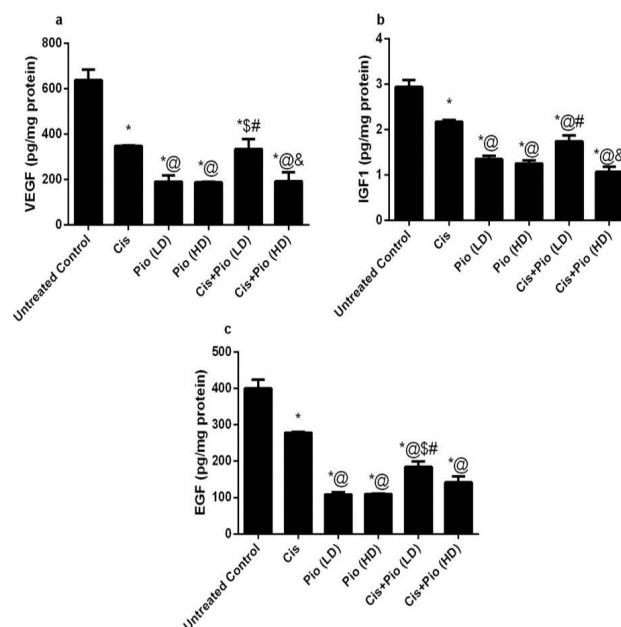

Figure 4: Effect of pioglitazone on the growth factors of ESC-bearing mice. a.Vascular endothelial growth factor (VEGF), and b. Insulin-like growth factor 1 (IGF1), and c. Epidermal growth factor (EGF). Data are expressed as mean ± SD, one-way ANOVA followed by post hoc test Bonferroni test for ten mice in each group. * Significant from the untreated control group, @ Significant from the cisplatin group, $ Significant from the Pio (LD) group, # Significant from the Pio (HD) group, & Significant from the Cis+ Pio (LD) group, p<0.05.

PPAR-γ expression in the untreated control group was significantly lower than in the groups with cisplatin alone or combined with lower or higher pioglitazone doses. However, PPAR-γ expression levels in the Cis+Pio (HD) group were the highest among the treated groups (Fig (5) a).

This study showed that untreated controls and Pio (LD) groups had the highest levels of p-ERK ½, respectively. However, both Cis-treated and Cis+Pio (HD) had in-significantly different levels. Notably, the Cis+Pio (HD) group showed the lowest significant p-ERK ½ levels among the groups (Fig (5) b).

p38 MAPK levels were reported in this study to be the highest in the untreated control group and Pio (LD) group, Additionally, levels in the Cis-treated group were

lower than levels in the other combination groups. Levels p38 MAPK were significantly the lowest in the Cis+Pio (HD) group (Fig (5) c).
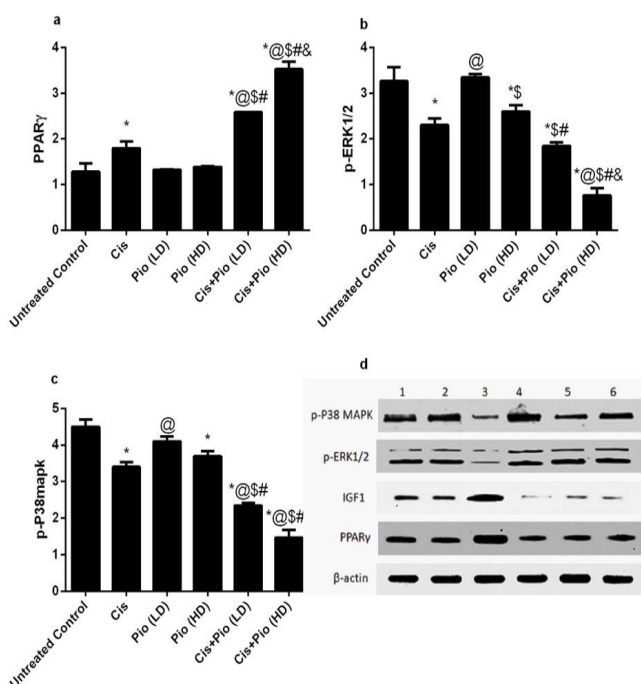

Figure 5: Effect of pioglitazone on the proliferation markers of ESC-bearing mice. a. Proliferating cell nuclear antigen (PPAR-γ), and b. Extracellular signal-regulated kinase (p-ERK ½), and c. p38 mitogen-activated protein kinase (p-38mapk). Data are expressed as mean ± SD, one-way ANOVA followed by post hoc test Bonferroni test for ten mice in each group. * Significant from the untreated control group, @ Significant from the cisplatin group, $ Significant from the Pio (LD) group, # Significant from the Pio (HD) group, & Significant from the Cis+ Pio (LD) group, *p*<0.05.
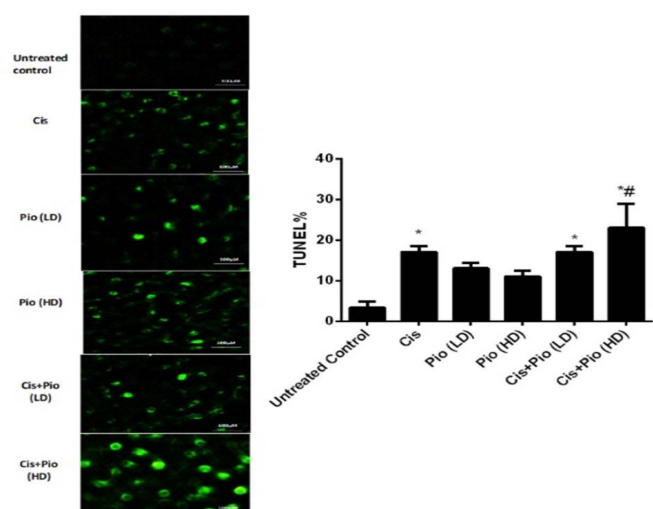

Figure 6: Effect of pioglitazone on the apoptotic activity of ESC-bearing mice using TUNEL assay Data are expressed as mean ± SD, one-way ANOVA followed by post hoc test Bonferroni test for ten mice in each group. * Significant

from the untreated control group, and # Significant from the Pio (HD) group, *p*<0.05.

EFFECT ON APOPTOSIS

Apoptosis TUNEL method was used in this study. The results revealed that pioglitazone in its low and high doses failed to significantly differ from the untreated control group. In contrast, cisplatin-treated group, Cis+Pio (LD) and Cis+Pio (HD) groups were significantly higher in the apoptotic activity compared to untreated controls (Fig. (6)).

HISTOPATHOLOGY AND IMMUNOHISTOCHEMICAL RESULTS

Tumor mass examination of the untreated control group revealed severely aggressive neoplastic cells arranged in solid patterns and sheets. The neoplastic cells showed malignancy criteria (hyperchromasia, pleomorphism, nucleus to cytoplasm ratio (1:1), haphazard arrangement, frequent atypical mitosis with numerous bizarre mitosis, and tumor giant cells formation). Also, it displayed severe anisokaryosis and anisocytosis accompanied by intense mononuclear cells infiltration and invasion of the adjacent muscle bundles, which suffered from hyaline degeneration, fragmentation, and necrosis. The other treated groups showed similar neoplastic cells; however, variable necrosis areas and apoptotic spaces were scattered among the tumor masses. Administration of cisplatin either alone or mixed with a lower or higher pioglitazone dose resulted in neoplastic replacement with newly formed fibrovascular granulation tissue in numerous examined sections of Cis, Cis + Pio (LD) and Cis + Pio (HD) groups (Fig (7)).
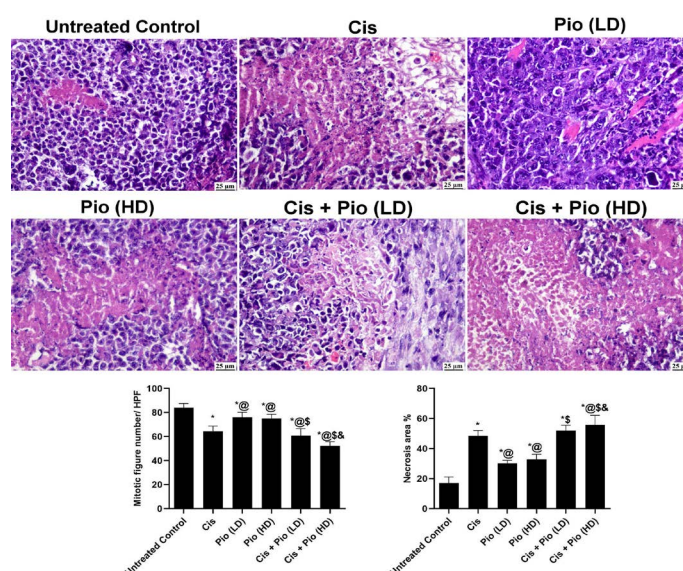

Figure 7: Histological sections stained with H&E showing the examined tumor mass in different groups.. The column charts illustrating the average of mitotic figure number/10 HPF and the necrosis area % in different groups. Data are expressed as mean ± SD, one-way ANOVA followed by

post hoc test Bonferroni. * Significant from the untreated control group, @ Significant from the cisplatin group, $ Significant from the Pio (LD) group, and & Significant from the Cis+ Pio (LD) group, $p<0.05$.

The mitotic figure and area percentage of necrosis were assessed in different groups. The mitotic figure count was significantly increased in the untreated control group compared to other groups. Cis + Pio (HD) showed the most remarkable improvement compared to other groups that showed a reduction by 37.85% and 20.4% in mitotic figure count compared to untreated control and Cis groups, respectively. Alternatively, the necrosis area % significantly decreased in the untreated control group compared to other groups. Co-administration of Cis and pioglitazone resulted in a significant increase in necrosis area % by 67.08% and 69.35% in Cis + Pio (LD) and Cis + Pio (HD) groups, respectively, compared to the untreated control group.

Immunohistochemical staining of PCNA, HIF-1α, PPAR-γ, and Cyclin D1 were investigated in different groups. The untreated group showed a significant increase in PCNA expression compared to other treated groups. There was no significant difference between the Cis and Cis + Pio (LD) groups. In contrast, a considerable reduction in the PCNA level positive cells was observed in the Cis + Pio (HD) group compared to other groups. Likewise, the untreated group showed a significant increase in the HIF-1α expression compared to other treated groups. A similar expression was noticed in all treated groups except for the Cis + Pio (HD) group, which scored a significant decrease compared to other groups (Fig (8)).
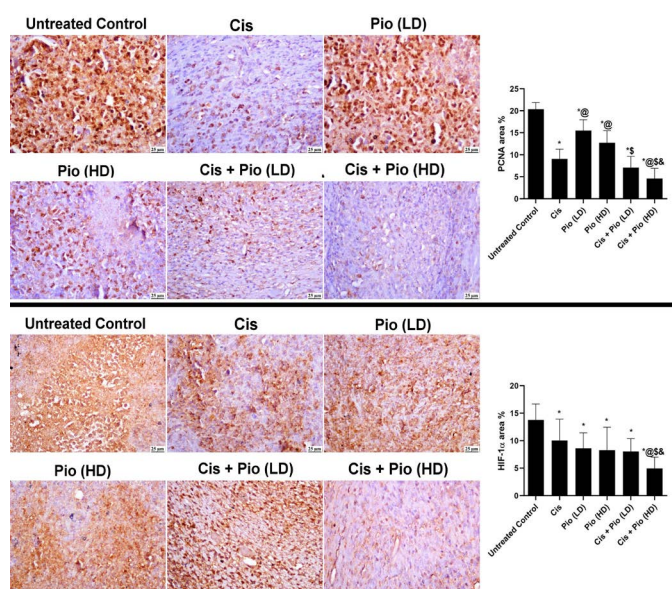

Figure 8: Histological sections immune stained with PCNA and hypoxia-inducible factor 1-alpha (HIF-1α) from solid tumor masses in different groups. Data are expressed as mean ± SD, one-way ANOVA followed by

post hoc test Bonferroni. * Significant from the untreated control group, @ Significant from the cisplatin group, $ Significant from the Pio (LD) group, and & Significant from the Cis+ Pio (LD) group, $p<0.05$.

Moreover, PPAR-γ expression was upregulated in the Cis + Pio (HD) group, which revealed a significant increase compared to other groups. Alternatively, the untreated control group exhibited a significantly weak expression of PPAR-γ compared to other groups. Regarding the immunostaining intensity of Cyclin D, there was remarkable positive staining in the untreated control group. However, few positive cells were detected in the Cis + Pio (LD) and Cis + Pio (HD) groups, which showed significant downregulation compared to other groups (Fig (9)).
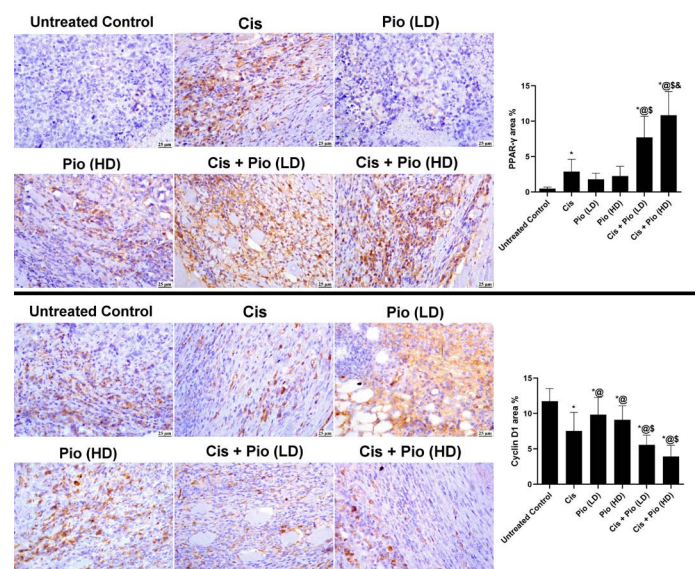

Figure 9: Histological sections immune stained with PPAR-γ and Cyclin D1 from solid tumor masses in different groups. Data are expressed as mean ± SD, one-way ANOVA followed by post hoc test Bonferroni. * Significant from the untreated control group, @ Significant from the cisplatin group, $ Significant from the Pio (LD) group, and & Significant from the Cis+ Pio (LD) group, $p<0.05$.

DISCUSSION

The current study not only focused on investigating the exact effect of Pioglitazone either alone or when combined with Cis but also, extended to underline its molecular mechanism on tumor microenvironment and the possibility of using pioglitazone as an adjuvant to lessen the possible side effects of chemotherapeutic agents in a well-established cancer model in mice. To the best of our knowledge this is the first study to report the actual role of pioglitazone on tumor angiogenesis and proliferation. Despite Various studies accentuated the anti-proliferative and anti-angiogenic effects of pioglitazone (Kole et al.,

2016; Ciaramella et al., 2019). Other studies highlighted an association between incidence of some cancer types and administration of Pioglitazone. (Piccinni et al., 2011) Therefore, it is not appropriate to pool the outcomes of the assorted studies as well as further observational research are needed to clarify the role of pioglitazone.

Chemotherapy is usually associated with sickness behavior that leads to discontinuation of the treatment protocol of cancer patients. This behavior is considered a consequence of either the disease itself or the chemotherapeutic medications and radiotherapy (Vichaya et al., 2016). ESC-bearing mice, Cis and Cis +Pio (LD)-treated mice displayed a reduced body weight, indicating increased sickness behavior. While mice treated with Pio (LD), Pio (HD), and Cis+(Pio HD) showed a relatively stable body weight compared to other groups indicating a less sickness behavior. This also was confirmed by recording their mortality rate throughout the experimental period. Cis treated group showed the highest percentage of mortality and this percentage decrease when combined with Pio (LD) and Pio (HD). The increased mortality rate in Cisplatin treated mice was due to the side effects of chemotherapy and not due to the ESC itself. The combination groups with Cis (Cis +Pio (LD) and Cis +Pio (HD)-treated mice seems to be effective in reducing the mortality rate compared to Cis treated group. Behavioral analysis, including the open field test and elevated plus-maze were further used to assess their locomotion and anxiety-like behavior. The untreated controls and Cis-treated mice exhibited a reduced locomotor activity and increased closed arm entries and duration. Taken together, these results indicate that Pio administration either alone or with Cis has an anxiolytic-like effect in reducing the sickness behavior of ESC-bearing mice. Different studies were conducted on rodents to explore the sickness behavior of chemotherapeutic agents, including Cis and doxorubicin, and the possible augmenting role of plant-based therapy (Orabi et al., 2021; Hamdan et al., 2022).

Moreover, mice treated with Cis+(Pio HD) displayed enhanced redox status by augmenting SOD, GSH, and reducing MDA levels, reflecting a more promising effect than Cis-treated mice. Several studies reported that the higher ROS levels in cancer cells cause further stimulation of the malignant phenotype, promoting sustained cell proliferation, cell survival, angiogenesis, metastasis, and inflammation. Therefore, oxidative stress is considered an established source of carcinogenesis (Buj and Aird, 2018). A higher oxidative stress state was reported to increase DNA damage and chromosomal aberrations and promote disease progression. This finding was consistent a recent study which demonstrated that cancer cell proliferation and survival were promoted through ROS-activated

pathways (Kabil et al., 2022). Additionally, a clinical trial showed that elevated MDA and ROS levels in patients treated with tyrosine kinases could indicate resistance to the treatment (Petrola et al., 2012).

Interestingly, mice treated with Cis+ (Pio HD) exhibited reduced levels of all tumor growth factors assessed in this study and was considered the lowest proliferation recorded in the treated experimental groups. The current findings were in the same line with Piątkowska–Chmiel and colleagues who used Pio to modulate chemotherapy resistance and reported the inhibited cell proliferation performed by Pio (Piątkowska-Chmiel et al., 2020). Also, Zarei et al. showed a reduced expression of VEGF in mice treated with pioglitazone. Consequently, the present results revealed a better antiproliferative effect when Pio is added to the standard chemotherapeutic treatment (Zarei et al., 2020).

Conversely, apoptosis rate was the best in mice treated with Cis or Cis+(Pio HD) group reflecting that pioglitazone did not reduce the apoptotic properties of cisplatin. These findings were inconsistent with Zhang and colleagues, who reported the nephroprotective effect of Pio against Cis renal toxicity through its antiapoptotic properties, which could be attributed to the higher dose used by the author (40 mg/kg) or the shorter study duration (seven consecutive days). (Zhang et al., 2020). Besides, Piątkowska-Chmiel and colleagues reported that Pio promoted tumor cell apoptosis and reduced cell viability when tested in the renal adenocarcinoma cell line (Piątkowska-Chmiel et al., 2020). Based on these data, the current study focused on investigating the exact effect of Pio either alone or when combined with Cis and extended to underline its molecular mechanism on tumor microenvironment and growth. In addition, Pio-treated groups displayed an elevated expression of PPAR-γ; therefore, when Pio is combined with Cis, a better-elevated expression of PPAR-γ was obtained. Following our findings, several experimental studies have reported the antitumor effect of PPAR-γ agonists. A recent study proposed that the nuclear receptor PPAR-γ has clinical potential as a pathological diagnostic, prognostic biomarker, and therapeutic target for glioblastoma (Hua et al., 2020). Kim and colleagues reported that in lung cancer, the antitumor effect of TZDs was mediated by PPAR-γ activation (Kim et al., 2015). Additionally, the activation of the PPAR-γ receptor was reported to protect cancer cells from the toxic effects of the platinum chemotherapy drug, Cis, by reducing metallothionein expression and inhibiting proteins that promote Cis resistance, such as promotion of the proliferation of the EGFR-TKI-resistant lung cancer cells (Heudobler et al., 2018).

In the current study our findings highlighted that pioglita-

zone, which is a PPAR-γ agonist, was able to increase the density of the receptor with Cis. These results were in the same line with Ni and colleagues, who showed the interplay between troglitazone and chemotherapeutic drugs Cis or paclitaxel' in xenotransplantation models indicating the chemotherapeutic drugs induction of PPAR-γ (Ni et al., 2017), in addition to the reported sequence-specific synergy between PPAR-γ ligands and chemotherapeutic agents in the treatment of cancer. Recent evidence shows that PPAR- agonists could serve as master modulators in the battle against cancer therapy's classic challenges, such as resistance to treatment and tumor genetic heterogeneity (Heudobler et al., 2018, Yousefnia et al., 2018, Zarei et al., 2020).

Furthermore, p-AMPK/ ERK ½ signaling pathways were inhibited by reduced p-AMPK, ERK1, and ERK2 in mice treated with the Cis+(Pio HD) group. ERK/MAPK signaling was reported as a fundamental pathway regulating cellular proliferation, differentiation, and survival. Moreover, activation of ERK/MAPK signaling pathways through phosphorylation activates other growth factor signaling pathways, including VEGF, platelet-derived growth factor, and EGF (Yuan et al., 2020). Besides, activating ERK/MAPK signaling pathway was reported in recent studies to increase tumor cells' resistance to chemotherapy. Rong and colleagues had shown that the ERK ½ signaling contributed to the tumor cellular resistance against cetuximab and considered EGFR/MAPK axis activation as a marker for bad prognosis (Rong et al., 2020). Another study reported reduced survival in cancer patients with elevated ERK1/2 phosphorylation levels. (Rong et al., 2019). The current findings consequently reflect the impact of Pio addition to Cis on increasing its efficacy and reducing resistance in addition to increasing survival rates.

These findings were confirmed by the histopathological investigation that highlighted the effect of Pio and the combined therapy in reduction of tumor growth through increased number of apoptotic spaces and necrotic areas with the further restoration of standard tissue architecture of adjacent muscle bundles by significant mitotic figures with subsequent reduction of invasion of the neoplastic cells. Furthermore, our result elucidated the role of Pio in combination with Cis in suppressing the proliferation of the neoplastic cells by decreasing the PCNA expression in a dose-dependent manner. PCNA marker plays a serious role in the cell cycle by raising the G1-S phases. (Tousson et al., 2011)

Furthermore, Pio-treated groups showed a marked decrease in HIF-1α expression, suggesting a potential mechanism in mitotic arrest in the proliferating neoplastic cells under hypoxic conditions. The increased expression of HIF-1α in tumor biopsies is often accompanied by an increased mortality rate in several types of cancer, including the bladder, oropharynx, breast, cervix, brain, endometrium, stomach, colon, lung, pancreas, and skin (Semenza, 2010).

Cyclin D1 regulates the cell cycle and promotes cells from G1-to S-phase. It phosphorylates pRb protein which acts as a nuclear phosphoprotein that controls cellular development in the G1-phase (Xu et al., 2013). In this study, Cyclin D1 expression was accompanied by a more favorable outcome in the Cis+ (Pio HD)-treated group than the untreated control and pioglitazone-treated groups. Overexpression of Cyclin D1 is investigated in many cancers related to progression and metastasis (Kabil et al., 2022).

CONCLUSION

This study provides a good framework for clinical trials evaluating the effectiveness of Pio as monotherapy or in combination with Cis anti-cancer compound in the treatment of human cancer. The current results demonstrated that the combined therapy of Pio and Cis was able to reduce sickness behavior in ESC-bearing mice and were demonstrated a superior antitumor, antiproliferative, antiangiogenic, antimitotic, and apoptotic activities as compared to monotherapy. In addition to the enhanced antioxidant activity of the combination rather than cisplatin alone, which generally reduced cellular injury and toxicity which indeed, provides preclinical evidence that this combined therapy may be considered as a promising therapeutic avenue for different cancer types. More experimental investigations are needed using different cancer models and chemotherapies, before it can be used in patients as an adjuvant agent to boost the therapeutic efficacy of chemotherapy in the treatment of many types of cancer.

ABBREVIATIONS

Abbreviations	Definitions
Cis	Cisplatin
EGF	Epidermal growth factor
ERK ½	Extracellular signal-regulated kinases
ESC	Ehrlich solid carcinoma
GSH	Glutathione
HD	High dose
HIF1-α	Hypoxia-inducible factor 1-alpha
IGF-1	Insulin like growth factor-1
LD	Low dose
MAPK	Mitogen-activated protein kinase
MDA	Malonaldehyde
PCNA	Proliferating cell nuclear antigen
Pio	Pioglitazone

PPARγ	Peroxisome proliferation-activated receptor
SOD	Superoxide dismutase
TZDs	Thiazolidinediones
VEGF	Vascular endothelial growth factor

FUNDING

DATA AVAILABILITY STATEMENT

All data used in this study are included in this published article.

CONFLICT OF INTEREST

All authors declared that there is no conflict of interest.

NOVELTY STATEMENT

The authors used the Ehrlich ascites carcinoma model to investigate the anti-tumor effect of two different doses of pioglitazone combined with one of the standard chemo-therapeutic agents (Cisplatin). This is the first study to look into this combination and pathway.

AUTHORS CONTRIBUTION

REFERENCES

Al-Eitan LN, Alzoubi KH, Al-Smadi LI, Khabour OF (2020). Vitamin E protects against cisplatin-induced genotoxicity in human lymphocytes. Toxicol *in vitro*. 62:104672. https://doi.org/10.1016/j.tiv.2019.104672

Ali MA, Khalil MM, Al-Mokaddem AK, Aljuaydi SH, Ahmed MM, Khalil HMA (2022). Differential effects of cancer modifying agents during radiation therapy on Ehrlich solid tumor-bearing mice: A comparative investigation of metformin and ascorbic acid. Appl Radiat Isot. 187:110305 https://doi.org/10.1016/j.apradiso.2022.110305.

Al-Muzafar HM, Amin KA (2018). Thiazolidinedione induces a therapeutic effect on hepatosteatosis by regulating stearoyl-CoA desaturase-1, lipase activity, leptin and resistin. Exp Ther Med. 16(4):2938-2948. https://doi.org/10.3892/etm.2018.6563

Bancroft J.D., Gamble M. (2013). Theories and practice of histological techniques. J. Clin. Pathol., 7(12): 2768-2773.

Bever SR, Liu X, Quan N, Pyter LM (2017). Euflammation Attenuates Central and Peripheral Inflammation and Cognitive Consequences of an Immune Challenge after Tumor Development. Neuroimmunomodulation. 24(2):74-86. https://doi.org/10.1159/000479184

Bray F, Ferlay J, Soerjomataram I, Siegel RL, Torre LA, Jemal A (2018). Global cancer statistics 2018: GLOBOCAN estimates of incidence and mortality worldwide for 36 cancers in 185 countries. CA Cancer J. Clin. 68(6):394-424 https://doi.org/10.3322/caac.21492.

Buj R, Aird KM (2018). Deoxyribonucleotide Triphosphate Metabolism in Cancer and Metabolic Disease. Front Endocrinol (Lausanne). 18;9:177. https://doi.org/10.3389/fendo.2018.00177

Choi J, Roberts LR (2016). Statins and metformin for chemoprevention of hepatocellular carcinoma. Clin. Liver Dis. (Hoboken). 29;8(2):48-52. https://doi.org/10.1002/cld.568

Ciaramella V, Sasso FC, Di Liello R, Corte CMD, Barra G, Viscardi G, Esposito G, Sparano F, Troiani T, Martinelli E, Orditura M, De Vita F, Ciardiello F, Morgillo F (2019). Activity and molecular targets of pioglitazone via blockade of proliferation, invasiveness and bioenergetics in human NSCLC. J. Exp. Clin. Cancer Res. 38(1):178. https://doi.org/10.1186/s13046-019-1176-1

Dana N, Vaseghi G, Haghjooy Javanmard S (2019). PPAR γ agonist, pioglitazone, suppresses melanoma cancer in mice by inhibiting TLR4 signaling. J. Pharm. Pharm Sci. 22(1):418-423. https://doi.org/10.18433/jpps30626

Ekinci Akdemir FN, Albayrak M, Çalik M, Bayir Y, Gülçin İ (2017). The Protective Effects of p-Coumaric Acid on Acute Liver and Kidney Damages Induced by Cisplatin. Biomedicines. 25(2):18. https://doi.org/10.3390/biomedicines5020018

Om-Ali Elkhawaga, Sara G, Nivin S (2019). Evaluation of anti-tumor activity of metformin against Ehrlich ascites carcinoma in Swiss albino mice, Egyptian J. Basic Appl. Sci. 1, 116-123 https://doi.org/10.1080/2314808X.2019.1676003

Ezzat M.I., Issa M.Y., Sallam I.E., Zaafar D., Khalil H.M., Mousa M.R., Sabry D., Gawish A.Y., Elghandour A.H., Mohsen E., (2022). Impact of different processing methods on the phenolics and neuroprotective activity of Fragaria ananassa Duch. extracts in ad-galactose and aluminum chloride-induced rat model of aging. Food Function., 13(14): 7794-7812. https://doi.org/10.1039/D2FO00645F

Gardouh AR, Barakat BM, Qushawy MKE, El-Kazzaz AY, Sami MM, Zaitone SA (2018). Antitumor activity of a molecularly imprinted nanopreparation of 5-flurouracil against Ehrlich's carcinoma solid tumors grown in mice: Comparison to free 5-flurouracil. Chem. Biol. Interact. 295:52-63. https://doi.org/10.1016/j.cbi.2018.04.019

Hamdan DI, El-Shiekh RA, El-Sayed MA, Khalil HMA, Mousa MR, Al-Gendy AA, et al (2020). Phytochemical characterization and anti-inflammatory potential of Egyptian Murcott mandarin cultivar waste (stem, leaves and peel). Food Funct.,11, 8214-8236 https://doi.org/10.1039/D0FO01796E

Hamdan DI, Tawfeek N, El-Shiekh RA, Khalil HMA, Mahmoud MY, Bakr AF, Zaafar D, Farrag N, Wink M, El-Shazly AM (2022). Salix subserrata Bark Extract-Loaded Chitosan Nanoparticles Attenuate Neurotoxicity Induced by Sodium

Arsenate in Rats in Relation with HPLC-PDA-ESI-MS/MS Profile. AAPS Pharm. Sci. Tech. 24(1):15. https://doi.org/10.1208/s12249-022-02478-4

Heudobler D, Rechenmacher M, Lüke F, Vogelhuber M, Pukrop T, Herr W, Ghibelli L, Gerner C, Reichle A (2018). Peroxisome Proliferator-Activated Receptors (PPAR)γ Agonists as Master Modulators of Tumor Tissue. Int. J. Mol. Sci. 19(11):3540. https://doi.org/10.3390/ijms19113540

Higuchi T, Sugisawa N, Miyake K, Oshiro H, Yamamoto N, Hayashi K, Kimura H, Miwa S, Igarashi K, Kline Z, Bouvet M, Singh SR, Tsuchiya H, Hoffman RM (2019). Pioglitazone, an agonist of PPARγ, reverses doxorubicin-resistance in an osteosarcoma patient-derived orthotopic xenograft model by downregulating P-glycoprotein expression. Biomed. Pharmacother. 118:109356. https://doi.org/10.1016/j.biopha.2019.109356

Higuchi T, Yamamoto J, Sugisawa N, Tashiro Y, Nishino H, Yamamoto N, Hayashi K, Kimura H, Miwa S, Igarashi K, Bouvet M, Singh SR, Tsuchiya H, Hoffman RM (2020). PPARγ Agonist Pioglitazone in Combination With Cisplatinum Arrests a Chemotherapy-resistant Osteosarcoma PDOX Model. Cancer Genom. Proteom. 17(1):35-40. https://doi.org/10.21873/cgp.20165

Hissin PJ, Hilf R (1976). A fluorometric method for determination of oxidized and reduced glutathione in tissues. Anal Biochem. 74(1):214-26. https://doi.org/10.1016/0003-2697(76)90326-2

Hua, T.N.M., Oh, J., Kim, S. et al (2020). Peroxisome proliferator-activated receptor gamma as a theragnostic target for mesenchymal-type glioblastoma patients. Exp. Mol. Med. 52, 629–642. https://doi.org/10.1038/s12276-020-0413-1

Kabil MF, Mahmoud MY, Bakr AF, Zaafar D, El-Sherbiny IM (2022). Switching indication of PEGylated lipid nanocapsules-loaded with rolapitant and deferasirox against breast cancer: Enhanced in-vitro and *in-vivo* cytotoxicity. Life Sci. ;305:120731. https://doi.org/10.1016/j.lfs.2022.120731

Khalil HMA, Eliwa HA, El-Shiekh RA, Al-Mokaddem AK, Hassan M, Tawfek AM, El-Maadawy WH (2021). Ashwagandha (Withania somnifera) root extract attenuates hepatic and cognitive deficits in thioacetamide-induced rat model of hepatic encephalopathy via induction of Nrf2/HO-1 and mitigation of NF-κB/MAPK signaling pathways. J. Ethnopharmacol. 277:114141. https://doi.org/10.1016/j.jep.2021.114141

Kim J, Sato M, Choi JW, Kim HW, Yeh BI, Larsen JE, Minna JD, Cha JH, Jeong Y (2015). Nuclear Receptor Expression and Function in Human Lung Cancer Pathogenesis. PLoS One. 10(8):e0134842. doi: 10.1371/journal.pone.0134842. https://doi.org/10.1371/journal.pone.0134842

Kole L, Sarkar M, Deb A, Giri B (2016). Pioglitazone, an anti-diabetic drug requires sustained MAPK activation for its anti-tumor activity in MCF7 breast cancer cells, independent of PPAR-γ pathway. Pharmacol Rep. 68(1):144-54. https://doi.org/10.1016/j.pharep.2015.08.001

Kubota N, Terauchi Y, Kubota T, Kumagai H, Itoh S, Satoh H, Yano W, Ogata H, Tokuyama K, Takamoto I, Mineyama T (2006). Pioglitazone ameliorates insulin resistance and diabetes by both adiponectin-dependent and-independent pathways. J. Biolog. Chem. 281(13):8748-55. https://doi.org/10.1074/jbc.M505649200

Lamontagne J, Jalbert-Arsenault E, Pepin E, Peyot ML, Ruderman NB, Nolan CJ, Joly E, Madiraju SR, Poitout V, Prentki M

(2013). Pioglitazone acutely reduces energy metabolism and insulin secretion in rats. Diabetes. 62(6):2122-9. https://doi.org/10.2337/db12-0428

Ni J, Zhou LL, Ding L, Zhao X, Cao H, Fan F, Li H, Lou R, Du Y, Dong S, Liu S, Wang Z, Ma R, Wu J, Feng J (2017). PPARγ agonist efatutazone and gefitinib synergistically inhibit the proliferation of EGFR-TKI-resistant lung adenocarcinoma cells via the PPARγ/PTEN/Akt pathway. Exp Cell Res. 361(2):246-256. https://doi.org/10.1016/j.yexcr.2017.10.024

Nishikimi, M., Appaji Rao, N. Yagi, K (1972). The occurrence of superoxide anion in the reaction of reduced phenazine methosulfate and molecular oxygen. Biochem. Biophys. Res. Commun. 46(2): 849–854. https://doi.org/10.1016/S0006-291X(72)80218-3

Noaman E, Badr El-Din NK, Bibars MA, Abou Mossallam AA, Ghoneum M (2008). Antioxidant potential by arabinoxylan rice bran, MGN-3/biobran, represents a mechanism for its oncostatic effect against murine solid Ehrlich carcinoma. Cancer Lett. ;268(2):348-59. https://doi.org/10.1016/j.canlet.2008.04.012

Ohkawa H, Ohishi N, Yagi K (1979). Assay for lipid peroxides in animal tissues by thiobarbituric acid reaction. Anal Biochem. ;95(2):351-8. https://doi.org/10.1016/0003-2697(79)90738-3

Orabi MAA, Khalil HMA, Abouelela ME, Zaafar D, Ahmed YH, Naggar RA, Alyami HS, Abdel-Sattar ES, Matsunami K, Hamdan DI (2021). Carissa macrocarpa Leaves Polar Fraction Ameliorates Doxorubicin-Induced Neurotoxicity in Rats via Downregulating the Oxidative Stress and Inflammatory Markers. Pharmaceuticals (Basel). 14(12):1305. https://doi.org/10.3390/ph14121305

Pantziarka P, Pirmohamed M, Mirza N (2018). New uses for old drugs. BMJ. 361:k2701. https://doi.org/10.1136/bmj.k2701

Petrola MJ, de Castro AJ, Pitombeira MH, Barbosa MC, Quixadá AT, Duarte FB, Gonçalves RP (2012). Serum concentrations of nitrite and malondialdehyde as markers of oxidative stress in chronic myeloid leukemia patients treated with tyrosine kinase inhibitors. Rev Bras Hematol Hemoter. 34(5):352-5 https://doi.org/10.5581/1516-8484.20120091.

Piątkowska-Chmiel I, Gawrońska-Grzywacz M, Natorska-Chomicka D, Herbet M, Sysa M, Iwan M, Korga A, Dudka J (2020). Pioglitazone as a modulator of the chemoresistance of renal cell adenocarcinoma to methotrexate. Oncol Rep. 43(3):1019-1030. https://doi.org/10.3892/or.2020.7482

Piccinni C, Motola D, Marchesini G, Poluzzi E (2011). Assessing the association of pioglitazone use and bladder cancer through drug adverse event reporting. Diabetes Care. 34(6):1369-71. https://doi.org/10.2337/dc10-2412

Reagan-Shaw S, Nihal M, Ahmad N (2008). Dose translation from animal to human studies revisited. FASEB J. 22(3):659-61. https://doi.org/10.1096/fj.07-9574LSF

Rong C, Muller M, Flechtenmacher C, Holzinger D, Dyckhoff G, Bulut OC, Horn D, Plinkert P, Hess J, Affolter A (2019). Differential Activation of ERK Signaling in HPV-Related Oropharyngeal Squamous Cell Carcinoma. Cancers (Basel). 11(4):584.. https://doi.org/10.3390/cancers11040584

Rong C, Muller MF, Xiang F, Jensen A, Weichert W, Major G, Plinkert PK, Hess J, Affolter A (2020). Adaptive ERK signalling activation in response to therapy and in silico prognostic evaluation of EGFR-MAPK in HNSCC. Br J. Cancer. 123(2):288-297. https://doi.org/10.1038/s41416-020-0892-9

Semenza GL (2010). Defining the role of hypoxia-inducible factor 1 in cancer biology and therapeutics. Oncogene. 4;29(5):625-34. https://doi.org/10.1038/onc.2009.441

Stehlik-Barry K., Babinec A.J. (2017). *Data Analysis with IBM SPSS Statistics*. Packt Publishing Ltd.

Tang H, Shi W, Fu S, Wang T, Zhai S, Song Y, Han J (2018). Pioglitazone and bladder cancer risk: a systematic review and meta-analysis. Cancer Med. 7(4):1070-1080. https://doi.org/10.1002/cam4.1354

Tousson E, Ali EM, Ibrahim W, Mansour MA (2011). Proliferating cell nuclear antigen as a molecular biomarker for spermatogenesis in PTU-induced hypothyroidism of rats. Reprod Sci. 18(7):679-86. https://doi.org/10.1177/1933719110395401

Vichaya EG, Molkentine JM, Vermeer DW, Walker AK, Feng R, Holder G, Luu K, Mason RM, Saligan L, Heijnen CJ, Kavelaars A, Mason KA, Lee JH, Dantzer R (2016). Sickness behavior induced by cisplatin chemotherapy and radiotherapy in a murine head and neck cancer model is associated with altered mitochondrial gene expression. Behav Brain Res. 297:241-50. https://doi.org/10.1016/j.bbr.2015.10.024

Wen W, Wu P, Gong J, Zhao M, Zhang Z, Chen R, Chen H, Sun J (2018). Association of Pioglitazone with Increased Risk of Prostate Cancer and Pancreatic Cancer: A Functional Network Study. Diabetes Ther. 9(6):2229-2243. https://doi.org/10.1007/s13300-018-0509-y

Xu C, Wu C, Xia Y, Zhong Z, Liu X, Xu J, Cui F, Chen B, Røe OD, Li A, Chen Y (2013). WT1 promotes cell proliferation in non-small cell lung cancer cell lines through up-regulating cyclin D1 and p-pRb in vitro and in vivo. PLoS One. 8(8):e68837. https://doi.org/10.1371/journal.pone.0068837

Yousefnia S, Momenzadeh S, Forootan FS, Ghaedi K, Esfahani MH (2018). The influence of peroxisome proliferator-activated receptor γ (PPARγ) ligands on cancer cell tumorigenicity. Gene. 649:14-22. https://doi.org/10.1016/j.gene.2018.01.018

Yuan J, Dong X, Yap J, Hu J (2020). The MAPK and AMPK signalings: interplay and implication in targeted cancer therapy. J Hematol Oncol.13(1):113. https://doi.org/10.1186/s13045-020-00949-4

Zarei R, Aboutorabi R, Rashidi B, Eskandari N, Nikpour P (2020). Evaluation of vascular endothelial growth factor A and leukemia inhibitory factor expressions at the time of implantation in diabetic rats following treatment with Metformin and Pioglitazone. Int. J. Reprod. Biomed. 18(9):713-722. https://doi.org/10.18502/ijrm.v13i9.7666

Zhang J, Zou Y, Cheng-Jing Y, Xiang-Heng L, Wang XP, Yu XJ, Li GS, Wang J (2020). Pioglitazone alleviates cisplatin nephrotoxicity by suppressing mitochondria-mediated apoptosis via SIRT1/p53 signalling. J. Cell Mol. Med. 24(20):11718-11728. https://doi.org/10.1111/jcmm.15782

Zhao XG, Sun RJ, Yang XY, Liu DY, Lei DP, Jin T, Pan XL (2015). Chloroquine-enhanced efficacy of cisplatin in the treatment of hypopharyngeal carcinoma in xenograft mice. PLoS One. 10(4):e0126147. https://doi.org/10.1371/journal.pone.0126147